

This document serves as supplementary to the paper titled 'Decoupled and Closed-loop Control of Motion and Stiffness for Articulated Soft Robots Driven by a Class of Electromechanical Variable Stiffness Actuators'.

Maja Trumić, *Member, IEEE*, Franco Angelini, *Member, IEEE*,
Kosta Jovanović, *Member, IEEE*, and Adriano Fagiolini, *Senior Member, IEEE*

This document serves as supplementary for the paper titled 'Decoupled and Closed-loop Control of Motion and Stiffness for Articulated Soft Robots Driven by a Class of Electromechanical Variable Stiffness Actuators'.

I. DERIVATION OF THE JOINT STIFFNESS EXPRESSION

This section presents the key calculations used to derive the joint stiffness expression considered in this paper. Similar derivations can also be found in previous works, including [1] and Chapter 21, Section 21.3.1 ("The Mass–Spring–Damper Paradigm") of the Handbook of Robotics [2].

We begin by considering a linear spring, that can store elastic energy U^e . Then, the force-displacement relation at equilibrium is described by

$$f(x) = \frac{\partial U^e(x)}{\partial x} \quad (1)$$

where f is the applied force and x is the corresponding displacement. The translational stiffness of this system is obtained by differentiating once more, i.e.

$$k(x) = \frac{\partial^2 U^e}{\partial x^2} = \frac{\partial f(x)}{\partial x}. \quad (2)$$

In our context, however, we are interested in the rotational counterpart of this formulation, as we deal with soft robots equipped with elastic, rotational joints. Here, torque and angular deflection take the place of force and linear displacement and we consider instead the so called rotational stiffness.

To elaborate this, let us consider an elastic deflection transmission connecting a motor to the driven link, as shown in Fig 1.

This work was supported by the EU under the Italian PNRR of NextGenerationEU, partnership on "Telecommunications of the Future" (PE00000001 - program "RESTART"), by the Science Fund of the Republic of Serbia, Green Program of Cooperation between Science and Industry, under Grant 6784, and by the Serbian Ministry of Science, Technological Development and Innovation (451-03-65/2024-03/200103 and 451-03-66/2024-03/200103).

Maja Trumić and Kosta Jovanović are with School of Electrical Engineering, University of Belgrade, Serbia (e-mail: {maja.trumic, kostaj}@etf.rs).

Franco Angelini is with Centro di Ricerca "Enrico Piaggio", and Dipartimento di Ingegneria dell'Informazione, Università di Pisa, Largo Lucio Lazzarino 1, 56122 Pisa, Italy (e-mail: franco.angelini@unipi.it).

Adriano Fagiolini, the corresponding author, is with MIRPALab, Department of Engineering, University of Palermo, Italy (e-mail: fagiolini@unipa.it).

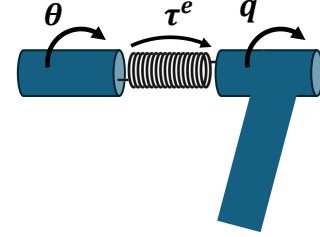


Fig. 1. Schematic representation of an elastic joint.

The angular deflection of the transmission is defined as $\phi = q - \theta$ where q is the joint position and θ is the motor position. This system stores elastic potential energy $U^e(\phi) \geq 0$ corresponding to the deflection ϕ , with $U^e(\phi) = 0$ if $\phi = 0$. The resulting elastic torque is expressed as

$$\tau^e(\phi) = \frac{\partial U^e(\phi)}{\partial \phi}, \quad (3)$$

and the rotational stiffness of the transmission is given by

$$\sigma(\phi) = \frac{\tau^e(\phi)}{\partial q} = \frac{\tau^e(\phi)}{\partial \phi} > 0. \quad (4)$$

Now consider an antagonistic actuation setup involving two motors—agonist and antagonist—acting on the same joint. The deflection transmission for each motor is $\phi_j = q - \theta_j$, where $j \in \{a, b\}$. The total potential energy stored in the elastic transmissions becomes:

$$U^e = \sum_j U_j^e(\phi_j),$$

as described in [3]. The corresponding total elastic torque applied to the joint is:

$$\tau^e(\phi_a, \phi_b) = \frac{\partial U_{e,a}(\phi_a)}{\partial \phi_a} + \frac{\partial U_{e,b}(\phi_b)}{\partial \phi_b} = \tau^e(\phi_a) + \tau^e(\phi_b) \quad (5)$$

and the total joint stiffness is

$$\sigma(\phi) = \frac{\partial \tau^e(\phi_a, \phi_b)}{\partial q} = \frac{\partial \tau^e(\phi_a)}{\partial \phi_a} + \frac{\partial \tau^e(\phi_b)}{\partial \phi_b}. \quad (6)$$

In the general case, we consider an n -degree-of-freedom articulated soft robot that has no elastic coupling between joints. Therefore, the elastic potential energy can be defined

for each joint individually. For the i -th joint the total elastic potential energy is $U_i^e = \sum_j U_{j,i}^e(\phi_{j,i})$. The total elastic torque for the i -th joint is

$$\tau_{j,i}^e = \tau_{a,i}^e + \tau_{b,i}^e = \frac{\partial U_{a,i}^e(\phi_{a,i})}{\partial \phi_{a,i}} + \frac{\partial U_{b,i}^e(\phi_{b,i})}{\partial \phi_{b,i}}, \quad (7)$$

and the corresponding i -th joint stiffness is

$$\sigma_i = \frac{\partial \tau_{a,i}^e}{\partial \phi_{a,i}} + \frac{\partial \tau_{b,i}^e}{\partial \phi_{b,i}}. \quad (8)$$

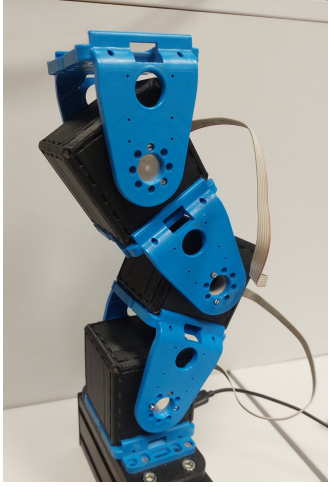


Fig. 2. A three degrees-of-freedom hardware setup used for the validation.

II. EXPERIMENTAL RESULTS FOR A THREE-DEGREE-OF-FREEDOM ARTICULATED SOFT ROBOT

To validate the control approach on a multi-DoF setup, we mounted an additional link to the robotic setup, thus adding

a degree of freedom to the previous robot such that the total number of degrees of freedom is equal to three, as shown in Fig. 2.

Again, the position and stiffness were commanded to follow the sinusoidal references. The trajectories are described as $q_{i,d} = \epsilon_{q_i} + A_{q_i} \sin \omega_{q_i} t$ and $\sigma_{i,d} = \epsilon_{\sigma_i} + A_{\sigma_i} \sin \omega_{\sigma_i} t$, for $i \in \{1, 2, 3\}$, where $\epsilon_{q_1} = 0.15$, $\epsilon_{q_2} = -0.3$, $\epsilon_{q_3} = 0.6$, $A_{q_1} = 0.1$, $A_{q_2} = 0.15$, $A_{q_3} = 0.15$, $\omega_{q_1} = \pi/15$, $\omega_{q_2} = \pi/7$, $\omega_{q_3} = \pi/7$, $\epsilon_{\sigma_1} = 11$, $\epsilon_{\sigma_2} = 10$, $\epsilon_{\sigma_3} = 7$, $A_{\sigma_1} = 1$, $A_{\sigma_2} = 1$, $A_{\sigma_3} = 2$, $\omega_{\sigma_1} = \pi/10$, $\omega_{\sigma_2} = \pi/8$, and $\omega_{\sigma_3} = \pi/8$. Intentionally, stiffness of the first two joints is set to a higher value such that these actuator are capable of supporting the robot structure. The corresponding control gains are $K_q \Lambda = \text{diag}_i \{4.9\}$, $K_q + \Lambda = \text{diag}_i \{0.7\}$, $K_\sigma = \text{diag}_i \{10\}$, $K_i = \text{diag}_i \{20\}$, $K_\pi = \text{diag}_i \{10\}$ and $\Delta = \text{diag}_i \{105\}$.

Figure 3 reports that the resulting positions, velocities and stiffness of all three joints converge to the desired trajectories, while the estimated parameters converge to the constant values. The figure also presents the commanded and achieved motor positions, as well as the corresponding tracking errors, which demonstrate smoothness of the input signals.

REFERENCES

- [1] F. Flacco and A. De Luca, "Stiffness estimation and nonlinear control of robots with variable stiffness actuation," *IFAC Proceedings Volumes*, vol. 44, no. 1, pp. 6872–6879, 2011.
- [2] B. Siciliano and O. Khatib, "Robotics and the handbook," in *Handbook of Robotics*. Springer, 2016, pp. 1–6.
- [3] R. Mengacci, F. Angelini, M. G. Catalano, G. Grioli, A. Bicchi, and M. Garabini, "On the motion/stiffness decoupling property of articulated soft robots with application to model-free torque iterative learning control," *The Int. J. Robot. Res.*, vol. 40, no. 1, pp. 348–374, 2021.

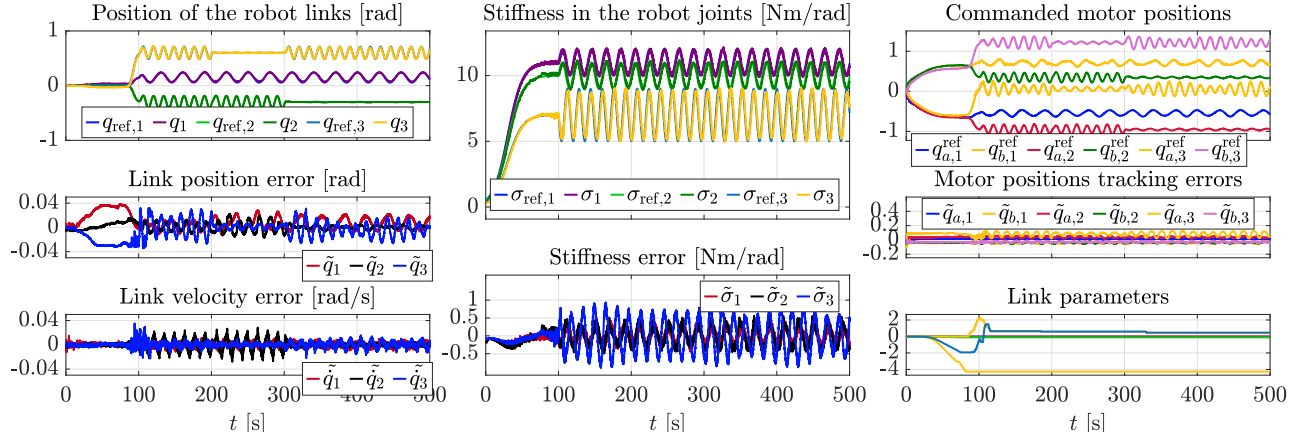


Fig. 3. The experiment on a three-DOF electromechanical articulated soft robot by using nonlinear adaptive control. All joint positions, velocities and stiffnesses are tracked accurately, while the parameters converge to constant values and the commanded motor positions have smooth behavior. The decoupling effect can again be observed in the leftmost figure, since the link positions and velocities remain constant despite the change of joint stiffness and other links motion.